Proceedings of the 9th U.S. National and 10th Canadian Conference on Earthquake Engineering
Compte Rendu de la 9ième Conférence Nationale Américaine et
10ième Conférence Canadienne de Génie Parasismique
July 25-29, 2010, Toronto, Ontario, Canada • Paper No 265

CYCLIC TRIAXIAL TESTING OF A WELL GRADED COMPACTED LIMESTONE ROCKFILL

H. Fallah[1]

ABSTRACT

The results of large scale static and cyclic triaxial tests for the Siah Bishe rockfill are presented. The test specimens are made of a modeled gradation with D_{max} of 5 cm, reduced by scalping method. Static triaxial tests resulted in the rockfill shear strength parameters within the expected range. The cyclic triaxial strength tests showed that the dam body rockfill failure criteria is not affected by earthquake loading. On the other hand, the cyclic triaxial parametric tests results were used to define shear modulus and damping curves of the compacted rockfill.

Introduction

The Siah Bishe pumped storage project, located 50 km northward of Tehran in central area of Alborz mountains, consists of two concrete face rockfill dams (CFRDs), whose main construction material is rockfill, from rock quarries. Therefore, the rockfill properties were determined by performing static and cyclic triaxial tests. The present article includes the results of the above mentioned tests for the Upper Dam, together with interpretation of the main results, including the rockfill shear strength parameters and shear modulus and damping curves. Triaxial tests were performed at Building and Housing Research Center (BHRC), Tehran, Iran.

Large Scale Cyclic Triaxial Testing

The present large scale cyclic triaxial testing facility is capable of testing cylindrical specimens with diameter of 300 mm and height of 600 m. Axial strain is measured by a linear variable differential transformer (LVDT) sensor with the capacity of 100 mm above the triaxial cell. Tests can be done via both stress and strain controlled methods. All stress paths in sinusoidal, rectangular, and triangular forms with frequencies from 0.1 Hz to 100 Hz could be applied to the specimen. Fig. 1 shows the general view of the triaxial testing facility.

Laboratory Specimens Preparation

When modeling a rockfill which its free draining property is important during design, scalping method is preferred to parallel gradation, in order to avoid increasing the fine content of

[1]Senior Geotechnical Engineer, Dept. of Hydropower, Poyry Energy AG - Iran

material, and to keep the high permeability of the rockfill (Varadarajan 2003). Therefore, scalping technique was used to scale the quarry rockfill size down to the lab size. According to this technique, from the in-situ curve, the materials larger than the lab maximum grain size are removed, and the reminder curve is scaled in which the lab D_{max} will become the D_{100} of the curve. For the present work, the fines content and the coefficient of uniformity ($C_u = D_{60}/D_{10}$) were kept changed (D_{60} and D_{10} were reduced with the same ratio) to have the modeled rockfill more similar to the real rockfill.

Figure 1. Cyclic triaxial testing facility at BHRC.

The in-situ gradation curve of the rockfill is taken as the mean curve of the material produced at quarry I, illustrated on Fig. 2. The triaxial apparatus available in BHRC is capable of testing specimens 300 mm in diameter. Therefore, the D_{max} of the modeled rockfill was set as 50 mm. The in-situ and modeled gradation curves are both presented on Fig. 2**.** The cylindrical specimens were made from the modeled rockfill, with the following conditions:

- diameter: 30 cm - height to diameter ratio: 2
- largest particle size: 5 cm
- compacted dry density: 2.10 gr/cm^3, equivalent to void ratios of 28.5 to 30 %

Within the methods of reconstituting specimens, moist vibration and moist tamping methods are applicable for coarse materials, which the second one was used. In this procedure, the moist material (with 4 to 5 percent moisture) is compacted in 6 to 7 lifts in a membrane lined split mold attached to the bottom platen of the triaxial cell. For each lift, the preweighed material is compacted by a tamper with a compaction foot to obtain the prescribed density. The lift surface should be uneven or rough, before placement of the next lift. To obtain layers with equal densities the bottom layers should be slightly undercompacted, since compaction of each succeeding layer densifies the layers below it. After the last layer is partially compacted, the top cap is put in place and vibration continued till the desired dry unit weight is obtained.

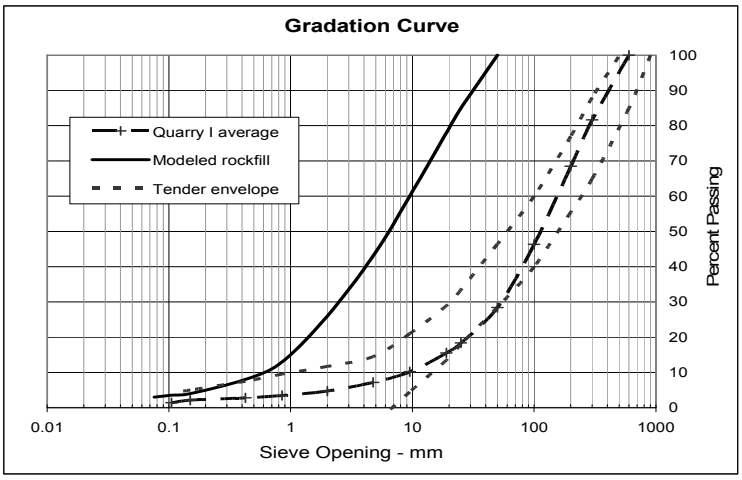

Figure 2. Modeled rockfill gradation curve.

Static Triaxial Tests Results

Mohr-Coulomb diagram of the static triaxial tests is illustrated in Fig. 3. The shear strength of rockfill is expressed in terms of a stress-dependent friction angle:

$$\phi' = \phi_0' - \Delta\phi' \log\left(\frac{\sigma_n'}{P_a}\right) \tag{1}$$

in which σ_n' is normal stress in MPa, and P_a is the atmospheric pressure (0.1 MPa). Thus, ϕ_0' is the friction angle corresponding to $\sigma_n' = p_a$ and $\Delta\phi$ is the reduction of the friction angle for every ten-fold increase of the confining stress. Variation of the friction angle as a function of normal stress is shown on Fig. 4. A trend line is fitted to the results, with $\phi_0' = 49.1°$, and $\Delta\phi = 8.6°$. The relatively high value of $\Delta\phi$ shows that the rockfill material from quarry I encounters a relatively high reduction in the friction angle with increasing normal stress.

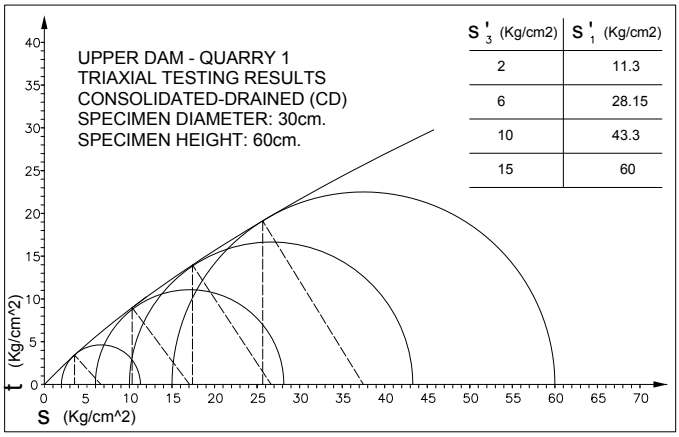

Figure 3. Mohr-Coulomb Diagram of modeled rockfill.

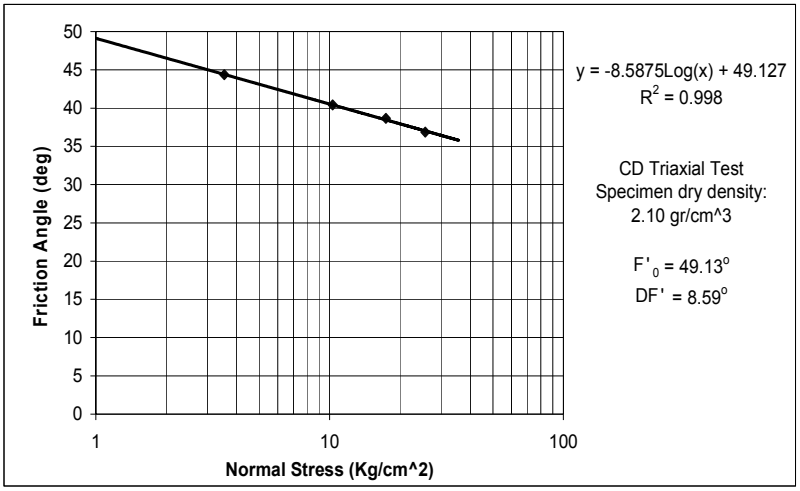

Figure 4. Variation of the compacted rockfill friction angle v.s normal stress.

Cyclic Triaxial Strength Tests Results

Cyclic Resistance of Coarse Grained Soils

One of the earliest endeavours in this context was made by Wong et al. (1975) who performed a series of cyclic triaxial tests on reconstituted specimens of gravely soils with different gradations by means of a large size triaxial apparatus. More recently, an attempt was made by Kokusho et al. (1995) on a volcanic debris deposit containing gravels. The block samples recovered by the ground freezing technique were cut into cylindrical specimens 30 cm in diameter and 60 cm in length and tested by using the triaxial test apparatus.

In the above efforts, because of the high stiffness of dense gravely soils, the double amplitude of 5% was difficult to be achieved. Therefore, the double amplitude of 2% was taken as a criterion to identify the state of cyclic softening. The tests results performed on dense gravely deposits indicate high cyclic strength ratio of the order of 0.3 to 0.5. For the present case, double amplitude of 2% was taken as the cyclic softening criterion, similar to dense gravely soils.

The Equivalent Number of Cycles Concept, and Cyclic Strength

Earthquake shaking is highly variable and irregular which in turn causes highly variable and irregular shear stresses in the ground, while laboratory tests are usually performed by the application of uniform stress cycles. Therefore, to make use of laboratory test data in an earthquake analysis, it is necessary to interpret an irregular shear stress record in terms of an equivalent number of uniform stress cycles. Seed et. al. (1975) set the uniform cyclic shear amplitude to 65% of the peak shear stress in the irregular time history. In the equation form:

$$\tau_{cycle} = 0.65\tau_{peak} \qquad (2)$$

Seed also studied actual ground motions and the resulting increase in pore pressures, and then correlated this with the number of $0.65\tau_{max}$ uniform stress cycles that produced similar pore pressures. The end result is presented in Fig. 5.

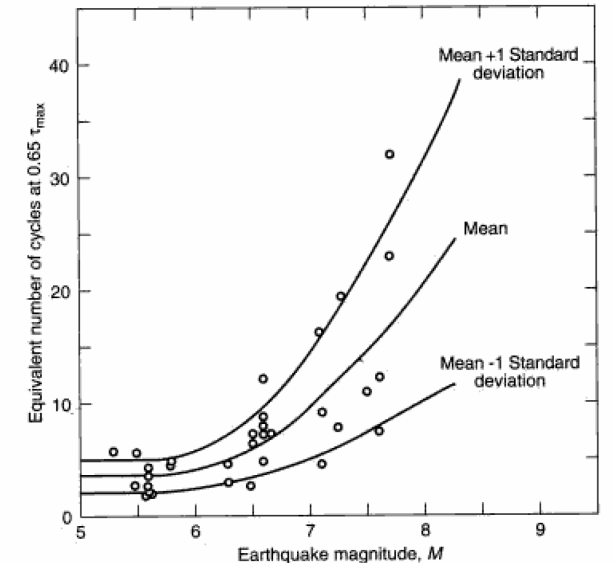

Figure 5. Equivalent uniform cycles versus earthquake magnitudes (after Seed et al., 1975).

Ishihara (1996) states that, it has been customary to consider 10 or 20 cycles in view of the typical number of significant cycles being present in many of actual time histories of accelerations recorded during past earthquakes. Therefore, he concludes that the onset condition of liquefaction or cyclic softening is specified in terms of the magnitude of cyclic stress ratio required to produce 5% double amplitude axial strain (or 2% for dense gravely soils) in 20 cycles of uniform load application.

Cyclic Strength Envelope from the Present Tests Results

The magnitude of cyclic load is determined from the desired stress ratio, SR:

$$SR = (\Delta\sigma_a)/(2\sigma'_{3c}) \quad (3)$$

where:
$\Delta\sigma_a$ = cyclic deviatoric axial stress
σ'_{3c} = consolidation pressure (chamber pressure minus back pressure)

The main results are presented in Table 1. In this table, N_L is the initial liquefaction cyclic number, and N=10 is the equivalent number of cycles. The results at N=10 are presented to illustrate the likelihood of initial liquefaction or cyclic softening of the tested sample. The results show that no considerable change happens to the specimens as a cause of cyclic loading, when the stress ratio is less than 0.30. Even with the stress ratios of 0.30 and 0.40 the initial liquefaction happens after a few hundreds of cycles. At the test No. 5, the pore pressure ratio reached the maximum value of 0.86 at the last loading cycle (No. 844), and N_L is estimated by

extrapolation. Only with the stress ratio of 0.45 the specimen has experienced a rapid increase in seismic pore pressure, reaching the initial effective confining pressure at cycle No. 14.

Table 1. Cyclic strength tests main results.

NO.	Consolidation pressure (kPa)	Stress ratio (SR)	Liquefaction cyclic number (N_L)	DA axial strain (%)			Seismic pore pressure ratio		
				N=10	N_L	N_{max}	N=10	N_L	N_{max}
1	200	0.10	-	0.019	-	0.020 (500)	0.007	-	0.025 (500)
2	200	0.20	-	0.100	-	0.100 (492)	0.037	-	0.190 (492)
3	600	0.20	-	0.106	-	0.110 (640)	0.188	-	0.470 (640)
4	600	0.30	310	0.160	0.640	-	0.128	1.0	-
5	600	0.40	≈ 1200	0.215	≈0.30	-	0.342	1.0	-
6	1000	0.45	≈ 14	1.312	1.85	-	0.883	1.0	-

The graph of cyclic resistance ratio versus number of uniform applied loading cycles is plotted in Figure 6. This graph, which is referred to as the *cyclic strength envelope*, is drawn by using the results of the tests No. 4, 5, and 6, with the stress ratios equal to or more than 0.3. The arrow on the last point indicates that the test represented by the data point has not reached the initial liquefaction condition at cycle No. 844, but is close to that. By using the Seed et. al. (1975) data and assuming the earthquake magnitude of 7, the corresponding equivalent uniform number of cycles is 10, which gives the cyclic strength of 0.44 using Figure 4. On the other hand, taking the equivalent uniform number of cycles of 20 (as suggested by Ishihara) results in the cyclic strength of 0.42, which is still quite a high cyclic strength value. In general, the modelled rockfill specimens are not considerably affected by cyclic loading, as expected from a well graded compacted rockfill material. Specially, cyclic softening is improbable.

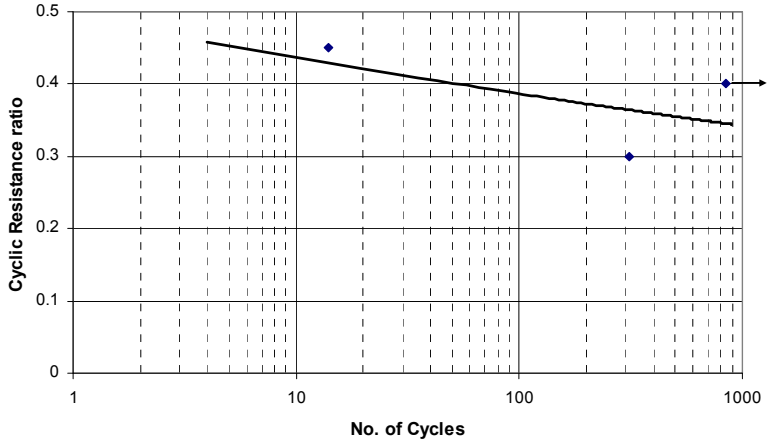

Figure 6. Cyclic resistance ratio versus number of loading cycles.

Seismic Pore Pressure Behavior

The pore pressures generated during earthquake shaking are a function of the earthquake magnitude which is reflected in the equivalent number of uniform cycles N, and on the other hand the soil condition which is represented by N_L. For stress controlled cyclic tests with uniform loading, Lee and Albaisa (1974) and De Alba et. al. (1975) found that the pore pressure r_u is related to the number of loading cycles N as:

$$r_u = \frac{1}{2} + \frac{1}{\pi}\sin^{-1}\left[2\left(\frac{N}{N_L}\right)^{1/\alpha} - 1\right] \qquad (4)$$

in which α is a function of the soil properties and test conditions.

Fig. 7 shows the data of the tests No. 4, 5 and 6. The De Alba et. al. (1975) function with α set to 1.0 is also added, for comparison. The polynomial curve fitted to the measured data shows a faster pore pressure build up during initial loading cycles. This is attributed to the behavior of dense rockfill under cyclic loading, in which the seismic pore pressure rises up more rapidly than the double amplitude strain, and cyclic softening or cyclic mobility is not the case.

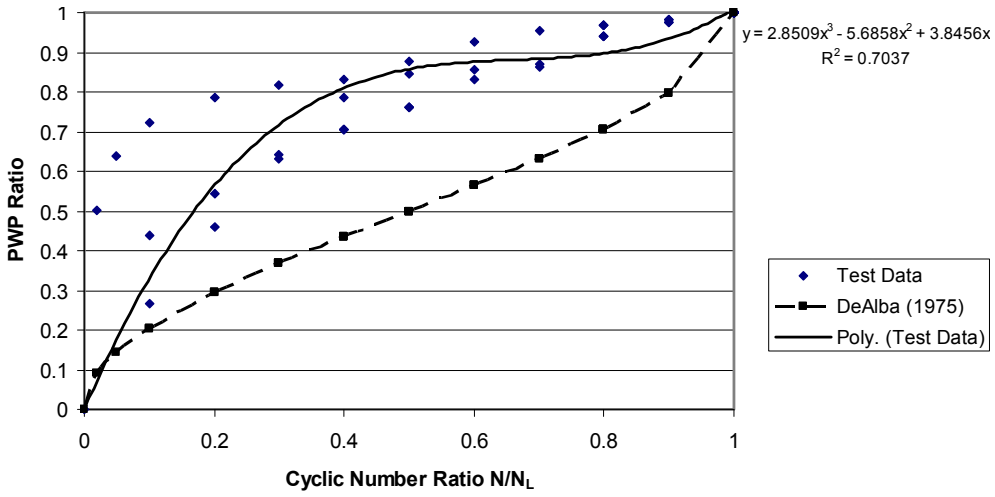

Figure 7. Cyclic number ratio N/N_L versus pore water pressure ratio r_u.

Cyclic Triaxial Parametric Tests Results

The cyclic part was done by constant cyclic load method and the magnitude of cyclic load was estimated for each stress ratio from Eq. 2. Six tests were performed after consolidating the specimens to consolidation pressures of 100, 200, 400, 600, 1000 and 1500 kPa.

Maximum Dynamic Shear Modulus

Because of the lack of large scale resonant column tests facility, it was decided to estimate the maximum dynamic shear modulus (at very small shear strain) by the available

correlations, and then adjust the estimation to fit to the tests results at higher strains. The maximum dynamic shear modulus G_{max} for coarse grain materials can be expressed as follows (Seed and Idriss, 1970):

$$G_{max} = 220\, k_{2max}\, (\sigma'_m)^{0.5} \quad \text{(in kPa)} \tag{5}$$

where k_{2max} is a material coefficient depending mainly on void ratio e (or relative density) and σ'_m is mean effective static stress. Values of k_{2max} for different gravely soils are shown in Fig. 8.

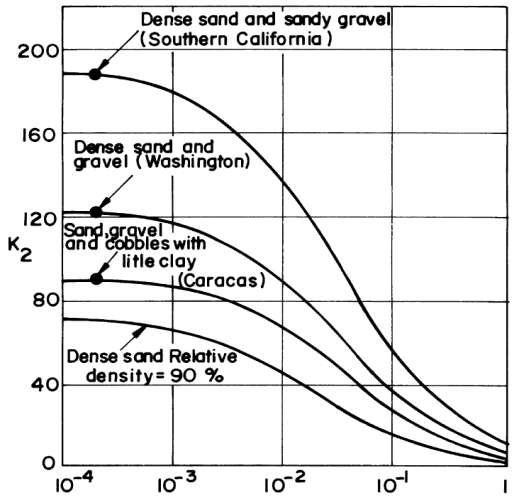

Figure 8. Values of k_{2max} for gravelly soils (Seed and Idriss 1970).

Calculation of the Shear Modulus from Young's Modulus

The Young's modulus for a given hysteresis loop is calculated as (Ishihara 1996):

$$\nu = (1 - nG_0C_l)/2 \tag{6}$$

where : n = porosity, %,
G_0 = maximum shear modulus, MPa, and
C_l = compressibility of water, 1/MPa.

By assuming $C_l = 4.85 \times 10^{-5}$ /MPa, the Poisson's ratio can be calculated as a function of porosity and maximum shear modulus. The calculated values vary from 0.454 to 0.489. Then, shear modulus is calculated from Young's modulus by the following formula:

$$G = E/2(1+\nu) \tag{7}$$

and shear strain is calculated from axial strain by the following relationship:

$$\gamma = (1-\nu)\varepsilon \tag{8}$$

Variation of Shear Modulus with Shear Strain

The shear modulus results with G/G_{max} format are illustrated on Fig. 9 with k_{2max} ranging from 90 to 115, together with the proposed range by Seed et al. (1984) for gravely soils. It can be seen that a new G/G_{max} range could be defined for the tested material, being representative of the well graded compacted limestone rockfill. The proposed range is also shown on Fig. 9.

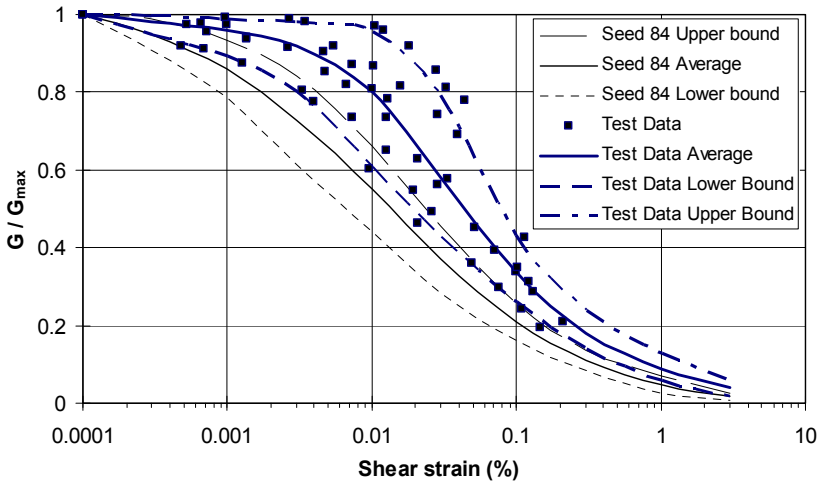

Figure 9. Variation of G/G_{max} with shear strain – well graded compacted limestone rockfill.

Variation of Damping Ratio with Shear Strain

Figure 10 shows the results of all the tests, together with the range proposed by Seed et al. (1984), for comparison. Based on this figure, damping ratios are increased at lower shear strains and decreased at higher shear strains, compared to the Seed et al. (1984) range. Therefore, a new damping range could be defined for the tested material, being representative of the well graded compacted limestone rockfill. The proposed range is also shown on Fig. 10.

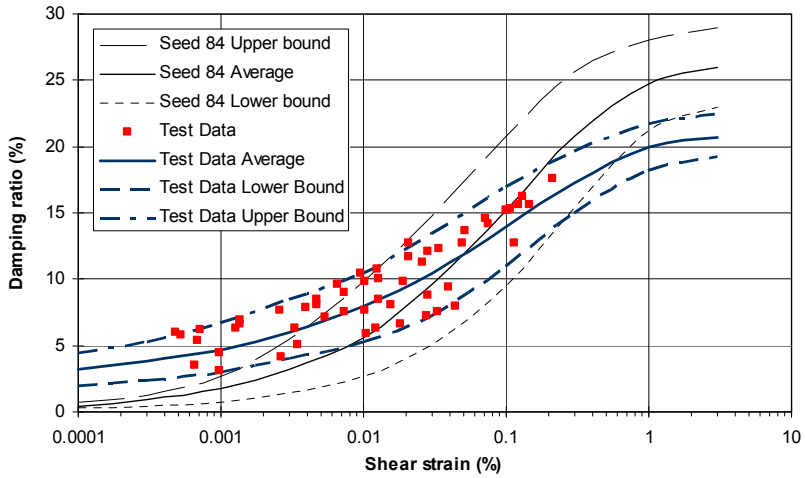

Figure 10. Variation of damping ratio with shear strain–well graded compacted limestone rockfill.

Conclusions

The well graded compacted rockfill is too strong to be considerably affected by cyclic loading. Cyclic softening or cyclic mobility is basically negligible for such a dense rockfill, even with high cyclic stress ratios. Based on the cyclic failure envelope defined by initial liquefaction (r_u = 1.0), the cyclic strength ratio of the rockfill is estimated between 0.42 to 0.44. Such high values above 0.3 indicate high resistance against liquefaction and strength reduction during earthquake.

For completion of the shear modulus variation curve, the G_{max} at shear strain of 10^{-6} is calculated by Eq. 5. The k_{2max} is estimated to adjust the G_{max} value to the curve passing the lab results, ranging from 90 to 115 for the 6 tests. The proposed range of G/G_{max} variation with shear strain is illustrated in Fig. 9, for the well graded compacted limestone rockfill.

Measured damping ratios are increased at low shear strains and decreased at high shear strains, compared to the range proposed by Seed et al. (1984). Therefore, a new damping range is defined for the tested limestone rockfill, illustrated in Fig. 10. All the above laboratory defined results are now the basis for final assessment of the dam static and dynamic stability analyses.

References

Varadarajan, A., K. G. Sharma, K. Venkatachalam, and A. K. Gupta, 2003. Testing and modeling two rockfill materials, *ASCE Journal of Geot. & Geo-environmental Engineering* 129 (3), 206-218.

Kokusho, T., Y. Tanaka, K. Kudo, and T. Kawai, 1995. Liquefaction case study of volcanic gravel layer during the 1993 Hokkaido Nonseioki Earthquake, *Proc. 3rd Int. Conf. on Recent advance in Soil Dynamics and Geot. Earthquake Eng., St. Louis* 1.

Wong, R. T., H. B. Seed, and C. K. Chan, 1975. Cyclic loading liquefaction of gravely soils, *ASCE Journal of Geotechnical Engineering* GT6, 571-583.

Seed, H. B., I. M. Idriss, F. Makdisi, and N. Banerje, 1975. Representation of irregular stress time histories by equivalent uniform stress series in liquefaction analyses, *Report No. EERC 75-29,* University of California, Berkeley.

Ishihara, K., 1996. *Soil behaviour in earthquake geotechnics,* Oxford science publications.

De Alba, P., C. K. Chan, and H. B. Seed, 1975. Determination of soil liquefaction characteristics by large scale laboratory tests, *Report No. EERC 75-14,* University of California, Berkeley.

Lee, K. L., and A. Albaisa, 1974. Earthquake induced settlements in saturated sands, *ASCE Journal of Soil Mechanics and foundation Division* 100, 387-406.

Seed, H. B., and I. M. Idriss, 1970. Soil Moduli and Damping Factors for Dynamic Response Analysis, *Report No. EERC 70-10,* University of California, Berkeley.

Seed, H. B., R. T. Wong, I. M. Idriss, and K. Tokimatsu, 1984. Moduli and Damping Factors for Dynamic Analyses of Cohesionless Soils, *Report No. EERC 84-14,* University of California, Berkeley.